Involvement of the posterior tool processing network during explicit retrieval of action tool and semantic tool knowledge: an fMRI study

Mathieu Lesourd, Emanuelle Reynaud, Jordan Navarro, Vivien Gaujoux, Alexandrine Faye-Védrines, Boris Alexandre, Josselin Baumard, Giovanni Federico, Franck Lamberton, Danielle Ibarrola, et al.

Involvement of the posterior tool processing network during explicit retrieval of action tool and semantic tool knowledge: an fMRI study

RUNNING TITLE: Posterior tool processing network and conceptual tool knowledge

Mathieu Lesourd[1], Emanuelle Reynaud[2], Jordan Navarro[2,3], Vivien Gaujoux[2], Alexandrine Faye-Védrines[2], Boris Alexandre[2], Josselin Baumard[4], Giovanni Federico[5], Franck Lamberton[6], Danielle Ibarrola[6], Yves Rossetti[7,8], & François Osiurak[2,3]

[1] Laboratoire de Recherches Intégratives en Neurosciences et Psychologie Cognitive & MSHE Ledoux, CNRS, Université Franche-Comté, F-25000, Besançon, France

[2] Laboratoire d'Etude des Mécanismes Cognitifs (EA 3082), Université Lyon 2, Bron, France

[3] Institut Universitaire de France

[4] Normandie Univ, UNIROUEN, CRFDP, Rouen, France

[5] IRCCS SDN, Naples, Italy

[6] CERMEP – Imagerie du vivant, MRI department and CNRS UMS3453, Lyon, France

[7] Centre de Recherche en Neurosciences de Lyon, Integrative, Multisensory, Perception, Action, & Cognition Team, Université de Lyon, France

[8] Mouvement, Handicap, et Neuro-Immersion, Hospices Civils de Lyon et Centre de Recherche en Neurosciences de Lyon, Hôpital Henry Gabrielle, St Genis Laval, France

Corresponding author :

Mathieu Lesourd


ORCID number : 0000-0002-1011-3047

Laboratoire de Recherches Intégratives en Neurosciences et Psychologie Cognitive
Université de Franche-Comté
19 rue Ambroise Paré
25030 Besançon Cedex
Email: mathieu.lesourd@univ-fcomte.fr

Manuscript word count (exc. figures/tables): 8917 words (5 figures/4 tables)

Abstract word count: 166 words

Abstract

Our ability to understand how to interact with familiar objects is supported by conceptual tool knowledge. Conceptual tool knowledge includes action tool and semantic tool knowledge which are supported by the ventro-dorsal and the ventral pathways, respectively. This apparent functional segregation has been recently called into question. In a block-design fMRI study, thirty-five participants were asked to complete manipulation, function, and association judgment tasks about pairs of familiar objects. Our results showed that lateral occipitotemporal cortex in the ventral pathway was more sensitive to manipulation and function judgment tasks compared to association judgement tasks. Functional connectivity analyses revealed distinct coupling patterns between inferior parietal lobule, lateral occipitotemporal cortex and fusiform gyrus. Taken together, these data indicate that action tool and semantic tool knowledge are both supported by ventral and ventro-dorsal pathways. Moreover, the explicit retrieval of these representations is supported by the functional coupling of common and distinct brain regions of the posterior tool processing network varying according to the kind of relations to be retrieved.

Keywords: association relations; explicit retrieval; fMRI; function relations; manipulation relations

1. Introduction

A defining characteristic of humans is the skillful use of tools to accomplish a task that would otherwise not be achievable (Ambrose 2001). The cognitive representations supporting the use of tools are underpinned by a predominantly left-lateralized brain network (Johnson-Frey 2004; Johnson-Frey et al. 2005; Lewis 2006; Gallivan et al. 2013; Ishibashi, Pobric, Saito, and Lambon Ralph 2016; Reynaud et al. 2016). This large brain network, hereafter called Tool Processing Network (TPN; see Garcea, Chen, Vargas, Narayan, & Mahon, 2018) is functionally organized according to the hypothesis of two segregated visuo-motor pathways: a ventral pathway ("what") which mediates semantic aspects of tools (i.e., semantic tool knowledge) and a dorsal pathway ("where"/"how") which mediates online control of object-directed actions (Ungerleider and Mishkin 1982; Goodale and Milner 1992). In a recent account of the two visuo-motor pathways, Binkofski and Buxbaum (2013) proposed an anatomical and functional subdivision of the dorsal pathway into a ventro-dorsal pathway (visual extrastriate cortex, angular gyrus, supramarginal gyrus, anterior intraparietal sulcus and ventral precentral gyrus) and a dorso-dorsal pathway (visual extrastriate cortex, posterior intraparietal sulcus, superior parietal lobe, and dorsal precentral gyrus). While the dorso-dorsal pathway is mainly involved in online monitoring of action (e.g., reaching/grasping; Rossetti et al., 2005; Tunik, Frey, & Grafton, 2005), the ventral and the ventro-dorsal pathways underpin the main representations about tool use. The ventral pathway supports semantic tool knowledge and the ventro-dorsal pathway supports action tool knowledge (Binkofski and Buxbaum 2013).

Semantic tool knowledge contains information about the prototypical use of familiar tools. When there are several possible ways of using a tool, they are likely to be weighted as a function of their familiarity and frequency (Goldenberg, 2013). Tool use depends on explicit semantic knowledge about usual tool-object relationships (i.e., association relations; a

hammer goes with a nail, or a hammer can be found in a garage) and tool function (i.e., function relations; a hammer and a mallet share the same purpose). Patients with lesions in the temporal lobes show deficits concerning semantic tool knowledge, particularly in function and association matching tasks (Baumard et al., 2016, 2019; Bozeat, Lambon Ralph, Patterson, & Hodges, 2002; Goldenberg & Spatt, 2009; Hodges, Bozeat, Lambon Ralph, Patterson, & Spatt, 2000; Lesourd et al., 2017). Imaging and stimulation studies in healthy participants have confirmed the role of ventral and lateral temporal regions in semantic tool knowledge (Boronat et al. 2005; Ebisch et al. 2007; Ishibashi et al. 2011, 2018; Andres et al. 2013; De Bellis et al. 2020).

Evidence has shown that semantic tool knowledge is neither necessary, nor sufficient for the actual use of tools (Buxbaum, Schwartz, & Carew, 1997; Negri, Lunardelli, Reverberi, Gigli, & Rumiati, 2007). In this regard, our ability to use tools is also based on action tool knowledge, allowing us to specify the action required to use a tool. Action tool knowledge might contain information about how to manipulate tools and is "thought to contain the features of gestures which are invariant and critical for distinguishing a given gesture from others" (Buxbaum, 2001, p.452). Other authors assume that action tool knowledge might contain information about physical principles (e.g., cutting, lever), which specify the mechanical action that must be performed (Osiurak & Badets, 2016; Osiurak, Jarry, & Le Gall, 2010, 2011; Osiurak, Lesourd, Navarro, & Reynaud, 2020). Debating this opposition is beyond the scope of the present study. For this reason, we will hereafter use the generic term action tool knowledge. Evidence has suggested that the inferior parietal lobule, and particularly the left supramarginal gyrus (SMG), might play a critical role in the processing of action tool knowledge. For example, patients with damage to the left inferior parietal lobule (IPL) classically show a deficit for using tools and pantomiming the use of tools (Goldenberg & Randerath, 2015; Martin et al., 2016, 2017; Niessen, Fink, & Weiss, 2014; Salazar-López, Schwaiger, & Hermsdörfer, 2016). The left AG also plays a role in determining adequate

hand posture to grasp a tool for subsequent use (Randerath et al. 2009, 2010). Imaging and stimulation studies in healthy participants contrasting manipulation judgment condition with either control condition or semantic tool tasks confirmed the role of the left IPL (in particular SMG) in action tool knowledge (Kellenbach et al. 2003; Canessa et al. 2008; Pelgrims et al. 2011; Andres et al. 2013; De Bellis et al. 2020).

To sum up, semantic tool knowledge when assessed with function and association judgment tasks relies upon the ventral pathway, whereas action tool knowledge when assessed with manipulation judgment tasks is mainly supported by the ventro-dorsal pathway. This apparent segregation between the cortical pathways supporting conceptual tool representations can be nevertheless questioned on several points. The first point concerns the specificity of the ventro-dorsal and the ventral pathways for action tool and semantic tool knowledge, respectively (i.e., one pathway supports one kind of representation). The second point concerns the exclusivity of the processing carried out in each pathway (i.e., there is no exchange of information between pathways during action tool and semantic tool retrieval). The third point is related to the apparent "unicity" of semantic tool knowledge (i.e., function and association relations share the same neurocognitive bases). These three points are now going to be discussed in turn in the following paragraphs.

Concerning the specificity of ventro-dorsal and ventral pathways for supporting action tool and semantic tool knowledge, numerous studies have shown that action tool knowledge is supported by both the ventro-dorsal pathway and the ventral pathway. Manipulation judgment tasks are frequently impaired in patients with damage to the ventral pathway, such as patients with semantic dementia, which concerns the ATL (Bozeat et al. 2002; Baumard et al. 2019). Lesions in the posterior part of the ventral pathway (i.e., left pMTG) have also been frequently associated with impaired performance in manipulation judgment tasks (Buxbaum, Shapiro, & Coslett, 2014; Kalénine & Buxbaum, 2016; Kalénine, Buxbaum, & Coslett, 2010; Martin et al., 2016; Tarhan, Watson, & Buxbaum, 2015). Conversely, it has been

demonstrated that semantic tool knowledge tapped onto the ventro-dorsal pathway, as brain imaging and brain stimulation studies revealed the involvement of the left IPL (De Bellis et al., 2018; Ebisch et al., 2007; Kellenbach et al., 2003; Kleineberg et al., 2018; for reviews see Binder, Desai, Graves, & Conant, 2009). To sum up, brain regions in ventral and ventro-dorsal pathway are involved in action tool and semantic tool knowledge.

The second point refers to the exclusivity of the processing carried out in each pathway. Indeed, the processing of action and semantic tool knowledge requires the interactions between ventral and ventro-dorsal pathways. The coupling between the two pathways have already been reported (for a review see Milner, 2017), particularly for object-related actions. For instance, Hutchison and Gallivan (2018) found a functional coupling between occipito-temporal and frontoparietal pathways for several sensorimotor tasks (e.g., grasp/reach task). The pantomime of tool use requires the activation of action tool knowledge (Buxbaum, 2014; Buxbaum, Kyle, Grossman, & Coslett, 2007; Buxbaum, Kyle, & Menon, 2005; Lesourd, Budriesi, Osiurak, Nichelli, & Bartolo, 2019; Niessen et al., 2014), and is associated with an increase functional connectivity between the left inferior LOTC and left IPL and left dorsal premotor cortex (Vingerhoets and Clauwaert 2015; Garcea et al. 2018). Consequently, action tool knowledge should also be supported by the coupling between ventral and dorsal pathways. Few studies have investigated the interactions between the two pathways for representations supporting tool use. Several studies pointed out that the left IPL gets input from ventral areas, therefore suggesting that object information was first processed in ventral areas and then combined with information coming from dorsal areas (Almeida, Fintzi, & Mahon, 2013; Mahon, Kumar, & Almeida, 2013; see also Lewis, 2006).

The third point concerns the “unicity” of semantic tool knowledge. Within semantic tool knowledge, function and association relations can be neurally dissociated, at least in part, within the ventral pathway (Schwartz et al. 2011; Mirman et al. 2017; Thye et al. 2021). While function relations call upon pMTG, ATL, and FG (Ishibashi et al. 2011, 2018; Chen et

al. 2016; De Bellis et al. 2020), association relations rather call upon pMTG and AG (Andres et al. 2013; Kleineberg et al. 2018). However, function relations, but not association relations, are impacted by virtual lesions in left LOTC and to a lesser extent in left SMG following virtual lesions occurring during the presentation of a manipulative prime (De Bellis et al. 2020). This suggests that function and manipulation relations may share close relationships, by assuming that a manipulative component may be embedded in function relations (for a discussion see Lesourd et al., 2021; see also Yee, Drucker, & Thompson-Schill, 2010). Taken together, these data suggest that manipulation and function relations share some neurocognitive similarities that function and association relations do not, calling into question the pure semantic nature of function relations. However, imaging studies that have contrasted manipulation and function conditions revealed a specificity for manipulation in left SMG, left IPS and bilateral pMTG (Kellenbach et al. 2003; Canessa et al. 2008; Kleineberg et al. 2018), whereas contrasting function and manipulation conditions has been rarely associated with significant activations (e.g., Boronat et al., 2005).

To date, no studies have investigated, in the same experimental design, the specific involvement and the interactions between brain regions of the TPN that support action tool and semantic tool knowledge, and more particularly manipulation, function and association relations. We aimed at filling this gap (1) by examining the modulation of posterior brain activity of the TPN, that is, in the left ventral temporal, left lateral temporal areas and left IPL, (2) by exploring the functional interactions between these areas during manipulation, function and association judgment tasks.

First, we aimed at testing several predictions concerning the involvement of posterior brain regions of the TPN in action tool and semantic tool tasks. The left SMG/IPS and the left LOTC have been associated with action tool representations, we then predict stronger activations for action tool (i.e., manipulation judgment task) compared to semantic tool tasks (i.e., association and function judgment tasks). We also predict stronger activations in

function compared to association judgment tasks, at least in the left LOTC. The left AG is often considered as a semantic node, involved in the retrieval of association knowledge (Binder et al. 2009; Kleineberg et al. 2018). Then, we should observe stronger activations in association compared to manipulation judgment task.

A secondary aim of the present study was to explore whether the functional interactions between the left IPL and the ventral and lateral temporal cortex were differentially modulated by manipulation, function and association judgement tasks. Even if naïve, the distinction between ventral and dorsal pathways has been proven to be useful before (e.g., Hutchison and Gallivan 2018; Kleineberg et al. 2018) and allows to make clear predictions. We hypothesize that explicitly retrieving action tool and semantic tool knowledge should be supported by the functional coupling between IPL and LOTC. We also expect that manipulation and function tasks may evoke similar pattern of functional connectivity between parietal and temporal regions compared to association tasks. Finally, functional connectivity should engage a wider network for manipulation compared to semantic tool tasks (i.e., association and function judgment tasks) in the posterior TPN.

2. Materials and Methods

2.1. Participants

Thirty-five healthy participants (M_{age} = 24.2, *SD* = 4.0, *range* = 18-36; 21 females; 34 right-handers) were enrolled in the study. Inclusion in the final sample required that head motion during scanning did not exceed 0.5mm displacement (i.e., framewise displacement) between consecutive volumes on 90% of volumes, however, no participants were excluded based on this criterion. All participants had normal or corrected-to-normal vision and reported no history of neurological or psychiatric disorder. All participants were volunteers and signed

written consent. The study was in line with the Declaration of Helsinki and was approved by the French Ethics Committee (N°ID-RCB: 2018-A00734-51). participants were paid for their participation.

2.2. Stimuli and Task

Three experimental conditions were used in the present study, namely, Manipulation condition, Function condition and Association condition. A set of 27 black colored line-drawings of uni-manually manipulable tools (targets) were used in the three conditions. In each condition, participants saw the picture of the target tool presented with either a related item or an unrelated item. We created a set of 71 unrelated items (27 x 3 conditions) and 71 related items (27 x 3 conditions). Thus, each condition was made by 54 pairs of items, half related pairs and half unrelated pairs (see **Supplementary Table 1**). In each stimulus, the two items were surrounded by a black frame and appeared on either side of a black cross presented on the center of the screen. Above each pair of items, a letter in upper case was depicted to indicate the condition.

In the Manipulation condition, the target tool (e.g., saw) was associated either with a tool being manipulated in the same way (e.g., iron; related pair) or not (e.g., faucet; unrelated pair). participants were asked to imagine if the two tools are manipulated in the same way. Here, participants did not have to focus on the hand posture but merely on the kinematic component. In the Function condition, the target tool (e.g., stapler) was associated either with a tool used for the same purpose (e.g., paper clip; related pair) or not (e.g., gas lighter; unrelated pair) and participants were instructed to imagine if the two tools were used for the same goal. Finally, in the Association condition, the target tool (e.g., bottle opener) was associated either with a situation where the target tool can be classically found (e.g., picnic; related pair) or not (e.g., runner; unrelated pair). Participants had to imagine if the target tool

can be found in the situation scene or not. A pretest was conducted in 15 participants who were not enrolled in the fMRI experiment. Participants were asked to judge the 54 pairs belonging to the manipulation condition, the 54 pairs belonging to the function condition, and the 54 pairs belonging to the association condition. A repeated measure ANOVA was conducted on raw scores with Task (3 levels = manipulation, function and association) as within factor. The ANOVA showed a significant effect of Task, $F(2,28) = 36.95$, $p < .001$, $\eta_p^2 = 0.73$, performance was better for association pairs ($M = 49.2$, $SD = 2.3$) compared to function pairs ($M = 44.7$, $SD = 4.4$, $p < .001$) and manipulation pairs ($M = 39.7$, $SD = 5.3$, $p < .001$). Performance for function pairs was better ($M = 44.7$, $SD = 4.4$, $p < .001$) than for manipulation pairs ($M = 39.7$, $SD = 5.3$, $p < .001$).

Two control conditions, including 32 new pairs of unrelated items (see **Supplementary Table 2**), were also constructed, one for the Manipulation and Function conditions and one for the Association condition. For the control of Association condition (Control_Tool-Context), 16 new pairs of unrelated items were prepared with pictures of target tools and pictures of context used in the Association condition. For the control of Manipulation and Function conditions (Control_Tool-Tool), 16 new pairs of unrelated stimuli were prepared with pictures of target tools and pictures of tools used either in the Manipulation or in the Function conditions. For sake of clarity, Control_Tool-Tool and Control_Tool-Context conditions will be both referred to as Control conditions in the results section. No pairs used in the control conditions were previously seen in any of the experimental conditions. Each item pair of the control conditions has been prepared in such a way that half of the pair of items included at least one item with a significant colored black surface (e.g., gun grip), which was not the case on the other half pair of items. In the control conditions, participants were asked to explore the items to find the presence or not of a black colored surface on one of the two items. The presence of control conditions was indicated by a black circle appearing

above the pair of items (instead of the letter appearing in the experimental conditions). All pictures had a resolution of 960 x 720 pixels.

2.3. Procedure and design

Each participant was scanned in a single fMRI session containing two functional runs. The first functional run (815 volumes, duration = 19mn) included the present experiment, was followed by a second functional run containing a distinct experiment (not included in the present study). The session always started by the acquisition of an anatomical sequence lasting for about 8 minutes (see section 2.4. below).

Before entering the scanner, participants were familiarized with the tasks. Practice trials were proposed in all conditions, but the pairs used for Manipulation, Function and Association trials did not re-appear in the fMRI experiment to avoid learning effects. A blocked within-subject design was used with alternating systematically experimental blocks (duration = 24s, 28s or 32s) and baseline periods (19s) (see **Figure 1**). During each baseline period, participants were shown a white screen with a fixation cross. Items were blocked by condition (i.e., Manipulation, Function, Association, Control_Tool-Tool and Control_Tool-Context), with trials varying from 7 to 9 per block. Each stimulus duration was fixed and lasted for 4s. There was no inter-stimulus interval. Six blocks were presented per experimental conditions and six blocks for control conditions (i.e., 4 for Control_Tool-Tool and 2 for Control_Tool-Context), yielding a total of 24 blocks[1]. Although each block varied from 24, to 28, to 32 seconds, after completing all 24 blocks, the average block length was similar for each condition (28 seconds). The number of related and unrelated pairs of stimuli was the same for each experimental condition and was balanced across all the blocks of the

[1] Each condition (Manipulation, Function, Association, Control_OO, and Control_OC) appears every 8 blocks, this design being repeated 3 times for a total of 24 blocks.

experiment[2]. There was the same number of items per condition. The order of the stimuli was randomized, while the order of blocks was pseudo-randomized to ensure that the experimental blocks were homogeneously distributed across the run. In the scanner, stimuli were back-projected onto a screen (60 Hz frame rate, 1024 x 768 pixels screen resolution) via a LCD projector (LX 501, CHRISTIE) and viewed through a mirror mounted on the head coil. Image on the screen had a 36x24 cm size.

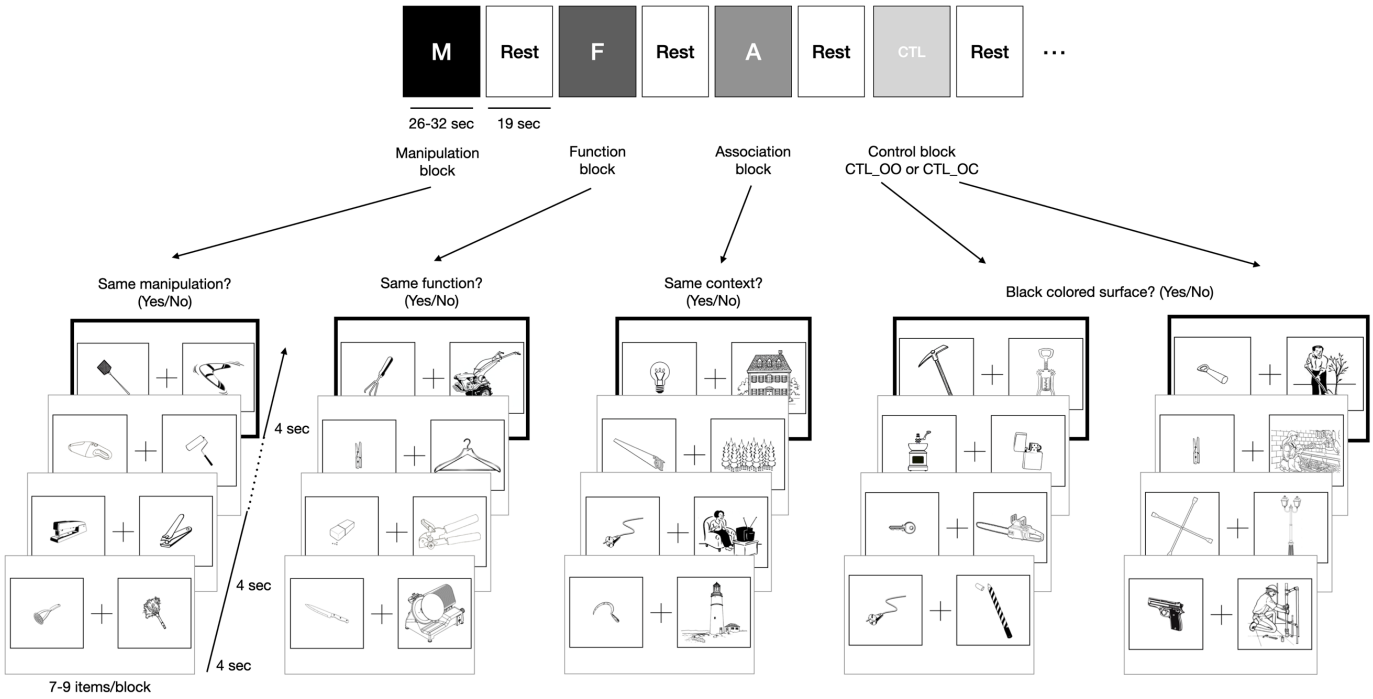

Figure 1. Experimental paradigm. Example of a block order in the beginning of a run (top). Schematic depiction of the sequence of trials in each experimental and control conditions (bottom).

Participants were asked to answer only on the last trial of a block, indicated by a red frame surrounding the whole item. This procedure was used to avoid confounding effects of motor execution on left and right hemispheric activations. Participants indicated their response by pressing one of two buttons with the thumb of their right hand and indicated a 'yes' response with the left button and a 'no' response with the right button. Participants were advised to remain attentive all along the block and to realize the task even if no response was expected.

[2] As a block contains 7, to, 8, to 9 items, related/unrelated pairs of stimuli could not be balanced within a block but were balanced across all the blocks of a given condition.

To ensure a sufficient level of attention on task, the number of trials was different across experimental blocks. The last item of each block (which was surrounded by a red frame), for which a motor response was produced, was not included in the analysis.

2.4. fMRI data acquisition

Imaging data were acquired on a 3T Siemens Prisma Scanner (Siemens, Erlangen, Germany) using a 64-channel head coil. Blood-Oxygen Level Dependent (BOLD) images were recorded with T2*-weighted echo-planar images (EPI) acquired with the multi-band sequence. Functional images were all collected as oblique-axial scans aligned with the anterior commissure–posterior commissure (AC–PC) line with the following parameters: 815 volumes per run, 57 slices, TR/TE = 1400 ms / 30 ms, flip angle = 70°, field of view = 96 x 96 mm^2, slice thickness = 2.3 mm, voxel size = 2.3 x 2.3 x 2.3 mm^3, multiband factor = 2. Structural T1-weighted images were collected using an MPRAGE sequence (224 sagittal slices, TR/TE = 3000 / 2.93 ms, inversion time = 1100 ms, flip angle = 8°, 224 x 256 mm FOV, slice thickness = 0.8 mm, voxel size = 0.8 x 0.8 x 0.8 mm^3).

2.5. Preprocessing of fMRI data

Structural T1-weighted images were segmented into tissue type (GM: grey matter, WM: white matter and CSF: cerebro-spinal fluid tissues) using the Computational Anatomy Toolbox (CAT12; http://dbm.neuro.uni-jena.de/cat12/) segmentation tool, in order to facilitate the normalization step. Functional data were analyzed using SPM12 (Wellcome Department of Cognitive Neurology, http://www.fil.ion.ucl.ac.uk/spm) implemented in MATLAB (Mathworks, Sherborn, MA). The first 3 EPI volumes were collected and discarded prior to the start by the scanner to allow for T1 equilibration effects. Preprocessing for univariate analyses included the following steps (1) 3D motion correction and linear detrending; (2)

realignment to the mean EPI image with 6-head motion correction parameters and unwarping using topup (Andersson et al. 2003); (3) co-registration of the individual functional and anatomical images; (4) normalization towards MNI template; and (5) spatial smoothing of functional images (Gaussian kernel with 5 mm FWHM).

2.6. Group analysis

A general linear model was created using design matrices containing one regressor (explanatory variable) for each condition (i.e., Manipulation, Function, Association, Control_Tool-Tool, and Control_Tool-Context) modeled as a boxcar function (with onsets and durations corresponding to the start of each stimulus of that condition) convolved with the canonical hemodynamic response function (HRF) as well as its temporal and derivatives dispersion. Six regressors of non-interest resulting from 3D head motion estimation (x, y, z translation and three axis of rotation) were added in the design matrix. The model was estimated in each participant, also taking into account the average signal in the run. After model estimation, we computed the three simple contrasts at the first level (i.e., experimental conditions against control conditions) that were transferred to a second level group analysis (one sample *t*-tests) to obtain the brain regions activated in the manipulation task (Manipulation > Control_Tool-Tool), in the function task (Function > Control_Tool-Tool) and in the association task (Association > Control_Tool-Context). Second, we entered maps of parameter estimates in a one-way ANOVA, with Task (Manipulation, Function, and Association) as within-subject factor, to identify brain regions where BOLD activity significantly differed across the three conditions. Moreover, ROI analyses with MarsBar ROI toolbox for SPM was used to extract parameter estimates in significant clusters showing a main effect of conditions (i.e., LOTC, AG, SMG/IPS) and in the 6 spherical ROIs (radius = 5mm) defined a priori from previous research on the topic (i.e., pFG, mFG, IPS, SMG,

pMTG, AG; see section 2.7.). Post-hoc (two-sided) t-tests were therefore used on mean parameter estimates. Third, maps of parameter estimates for Manipulation, Function and Association were also used to perform a conjunction analysis, which tests for areas activated in all conditions. We present results maps with a significance threshold set at $p < .05$ with family-wise error (FWE) correction for simple contrasts and with a more conservative threshold for ANOVA and conjunction analyses ($p < .01$).

2.7. Seeds selection

A total of 6 spherical seeds ROIs (radius = 5 mm) were created in the MNI atlas space (see **Table 1** and **Figure 2**). We focused our analysis on the left hemisphere, as the TPN is left lateralized in the brain (Lewis 2006; Ishibashi et al. 2016; Reynaud et al. 2016). To ensure the independence of ROI selection from ROI testing, we used literature-defined ROIs from previous research on representation supporting tool use and actual tool use (Chen et al., 2016; Kalénine & Buxbaum, 2016; Randerath et al., 2010; Reynaud et al., 2016). The selection of seeds (detailed in the next paragraph) was based on fMRI studies (activation peaks) and VLSM studies (overlap of lesioned voxels). The analysis was performed in the MNI space, thus coordinates reported in Talairach reference space (Talairach and Tournoux 1988) were first converted to MNI space using icbm2tal transformation (Lacadie et al. 2008) implemented in a webapp (https://bioimagesuiteweb.github.io/webapp/mni2tal.html).

Table 1. Seed-region locations

Seed name	Brodmann Area	MNI coordinates			Studies / method
		x	y	z	
Ventral pathway					
pMTG	BA19	-58	-65	3	Kalénine et al. (2016) / VLSM study
pFG	BA37	-44	-62	-14	Chen et al. (2016) / fMRI study (localizer)
mFG	BA37	-29	-52	-20	Chen et al. (2016) / fMRI study (localizer)
Ventro-dorsal pathway					
AG	BA39	-45	-66	37	Randerath et al. (2010) / VLSM study
IPS	BA40	-36	-50	46	Chen et al. (2016) / fMRI study (localizer)
SMG	BA40	-60	-34	46	Reynaud et al. (2016) / fMRI meta-analysis study

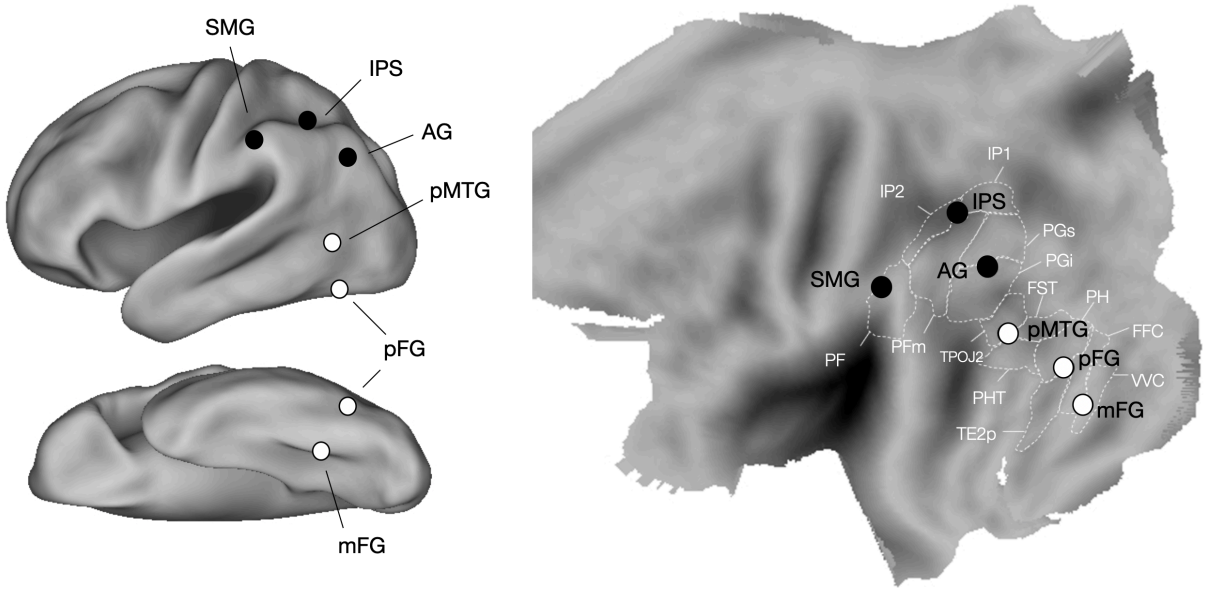

Figure 2. Seed ROIs in the posterior TPN. Locations of the 6 spherical seed ROIs (radius = 5mm) are projected on an inflated-map (left) and on a flat-map (right) representation of the left hemisphere of the PALS-B12 atlas surface configurations (Van Essen 2005). The parcellation is based on Glasser et al. (2016). For the abbreviations, see the main text and Appendix. ROIs within the ventral pathway are colored in white and ROIs in the ventro-dorsal pathway are colored in black. SMG: supramarginal gyrus; IPS: intraparietal sulcus; AG: angular gyrus; pMTG: posterior middle temporal gyrus; pFG: posterior fusiform gyrus; mFG: middle fusiform gyrus.

We defined each spherical seed in ventral and ventro-dorsal pathways that are both involved in the TPN:

- In left IPL, SMG supports the understanding of tool-object interactions (i.e., mechanical knowledge; Orban & Caruana, 2014; Reynaud et al., 2016). Lesions in AG have been associated with erroneous grasping of tools[3] (VSLM study; Randerath, Goldenberg, Spijkers, Li, & Hermsdörfer, 2010). Finally, IPS is a tool-sensitive region, which is involved in the planning of object-related actions (localizer in a fMRI study; Chen, Garcea, & Mahon, 2016).
- The LOTC supports both action and semantic tool representations. The left pMTG is involved in gesture recognition (VLSM study; Kalénine & Buxbaum, 2016). The

[3] The left AG is traditionally not included in the TPN, however this brain region which is part of the ventro-dorsal pathway is involved in semantic tool knowledge and in a lesser extent in action tool knowledge (Lesourd et al. 2021).

occipito-temporal cortex includes also tool-sensitive regions in mFG and pFG[4] (localizer in a fMRI study; Chen, Garcea, & Mahon, 2016).

2.8. ROI-to-ROI Functional connectivity analysis

Task-related ROI-to-ROI functional connectivity (FC) was analyzed with the SPM toolbox CONN (Whitfield-Gabrieli and Nieto-Castanon 2012). For each subject, first level SPM matrices estimated on functional images, normalized T1 images, and normalized segmentation of GM, WM and CSF were imported in CONN, as the 6 seed ROIs described in the previous section. An aCompCorr denoising process (Behzadi et al. 2007) was applied to remove confounds of white matter, CSF, subject motion and effects of the task. This procedure allows to remove the temporal time series of each confound from EPI images. Adding regressors accounting for task effects in this preprocessing step allowed preventing that the main effects of the task drove the estimation of the correlations quantifying FC. Finally, additional steps included detrending, despiking, and filtering ($0.008Hz < f < 0.09Hz$) to the residual time series. We used the option "Weighted GLM" offered in the CONN toolbox, in which each condition of interest was described by a boxcar function and convolved with a canonical hemodynamic response function (HRF). For each subject, average time series weighted per condition were extracted across all voxels within each ROI and bivariate correlation coefficients between each pair of ROIs considered in isolation were computed; these coefficients were then Fisher-transformed at the group-level and ROI-to-ROI FC was examined for each contrast, that is, Manipulation>Control_TT, Function>Control_TT, and Association>Control_TC. An average cross correlation matrix between all regions for each condition was then calculated. All group-level results were

[4] The pFG ROI of the present study was initially labelled pMTG in Chen et al. (2016), but as it is located in the inferior occipital gyrus, particularly in FG2/FG4, according to its cytoarchitectonic location (Anatomy toolbox; Eickhoff et al. 2005), we chose to label it posterior fusiform gyrus (pFG), as it can be found in the posterior part of the fusiform gyrus (probability for FG2: 53% and for FG4: 43%).

corrected for multiple comparisons (false discovery rate; FDR) at seed-level ($p_{FDR} < .05$) within the CONN toolbox.

3. Results

3.1. Behavioral data

To ensure that participants remained focused on the task all along the run, we analyzed judgment accuracies and RTs on Manipulation, Function and Association conditions for the last item of each block for which a response was done. We also reported separately the mean accuracy and mean RT for the control condition.

The ANOVA carried out on judgement accuracies revealed no main effect of Task, $F(2,68) = 1.68$, $p = .19$, $\eta_p^2 = 0.05$, the participants performed equally in Manipulation (M = 86.67%, SD = 15.55), Function (M = 92.38%, SD = 10.95), and Association conditions (M = 90.00%, SD = 12.26). However, the ANOVA carried out on RTs revealed a main effect of task, $F(2,68) = 33.10$, $p < .001$, $\eta_p^2 = 0.49$, Manipulation judgements (M = 2.31s, SD = 0.37) were slower than Function (M = 1.93s, SD = 0.32, $p < .001$) and Association judgments (M = 2.09s, SD = 0.36, $p < .001$), and Function judgments were slower than Association judgements ($p < .001$).

In the control condition, participants showed high accuracies (M = 95.24%, SD = 8.64) associated with short RTs (M = 1.63s, SD = 0.24).

3.2. GLM analysis

We first computed the simple contrasts Manipulation>Control, Function>Control and Association>Control (see **Figure 3** and **Table 2**). To control for multiple comparisons, we used cluster-based corrections which gave more lenient results, compared to voxel-based corrections. This procedure was used only for the analysis of the simple contrasts. Contrasting Manipulation condition with control condition revealed activations in bilateral temporo-

occipital fusiform cortex, bilateral precentral gyrus, bilateral insula, and in left IPL (SMG and IPS), left IFG and left dPMC. Contrasting Function condition with control condition led to significant activations in bilateral lateral occipital cortex, left IFG, and in left fusiform gyrus. Contrasting Association condition with control condition revealed activations in bilateral lateral occipital cortex and fusiform cortices, bilateral temporal pole, left IFG and in left superior temporal gyrus/middle temporal gyrus.

We also contrasted the control conditions between each other (see **Supplementary Figure 1** and **Supplementary Table 3**). Contrasting Control_OO with Control_OC did not reveal any significant activations, whereas contrasting Control_OC with Control OO led to significant activations in bilateral occipital pole, bilateral inferior lateral occipital temporal cortex, left lingual gyrus, and left temporal pole.

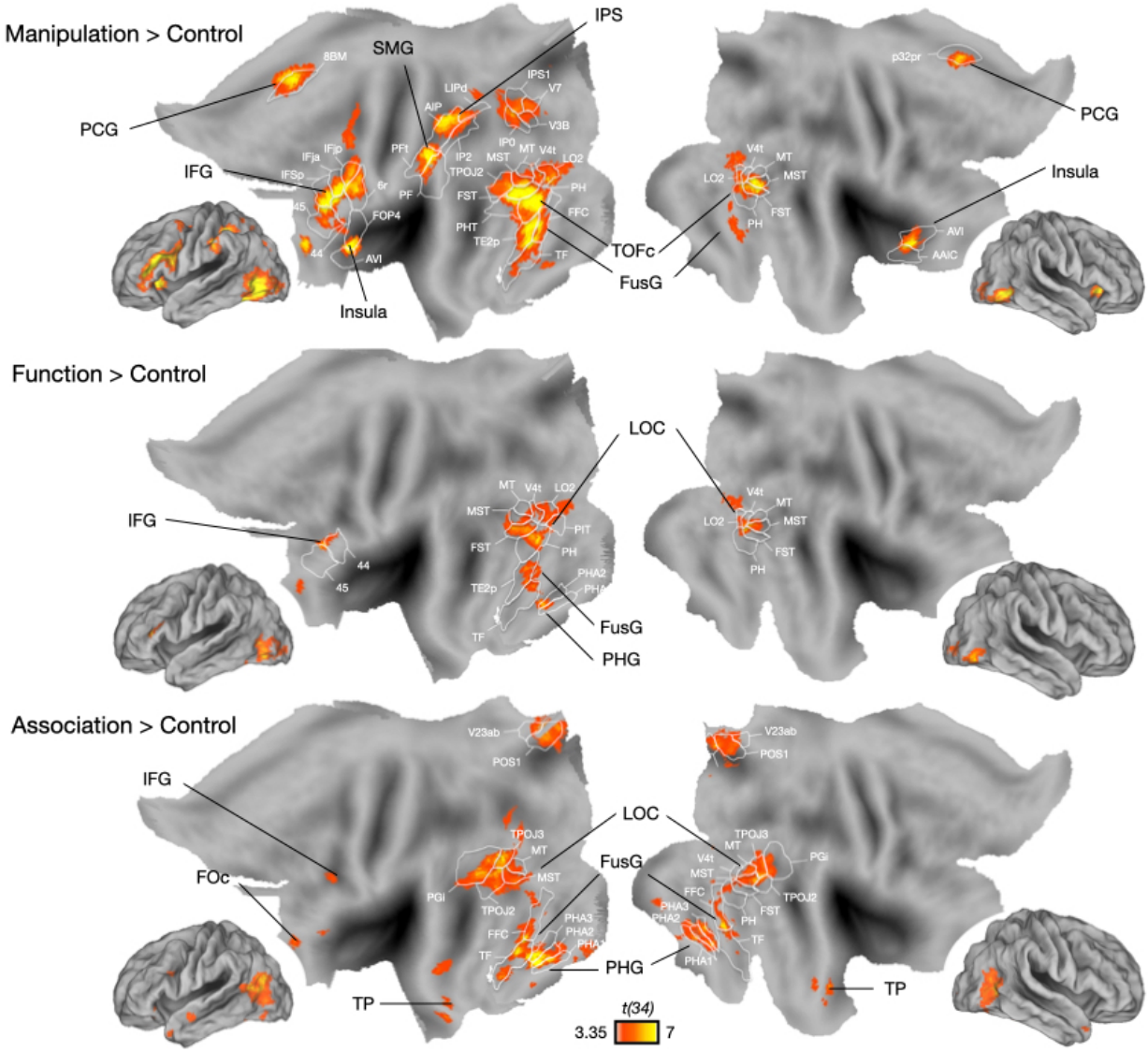

Figure 3. Statistical maps for the contrasts Manipulation>Control, Function>Control and Association>Control are projected on PALS-B12 atlas surface configurations (Van Essen 2005) and are FWE-corrected, [$t(34 > 3.35)$, $p < .05$] for multiple comparisons across the whole-brain at the cluster level (threshold of spatial extent: Manipulation = 69 voxels; Function = 46 voxels; Association = 67 voxels). The parcellation is based on Glasser et al. (2016). For the abbreviations, see Appendix. PCG: precentral gyrus; IFG: inferior frontal gyrus; SMG: supramarginal gyrus; IPS: intraparietal sulcus; TOFc: temporo-occipital fusiform cortex; FusG: fusiform gyrus; LOC: lateral occipitotemporal cortex; PHG: parrahippocampal gyrus; FOc: fronto-orbital cortex; TP: temporal pole.

Table 2. Local maxima of activation clusters (MNI stereotactic coordinates) for the individual contrasts Manipulation > Control, Function > Control, and Association > Control

Brain region	Hemisphere	Peak MNI coordinates			Cluster size	T-value	P_{FWE}
		x	y	z			
Manipulation > Control							
IFG *pt* / Insula	Left	-47	34	11	2417	10.74	<.001
FG / SMG / TOFc	Left	-38	-55	-12	3718	9.36	<.001
Cerebellum VIIb/VIII	Right	21	-73	-49	2544	9.14	<.001
PCG / SFG	Left/Right	-4	21	48	488	8.31	<.001
Insula	Right	35	25	-3	196	6.96	<.001
Function > Control							
Cerebellum Crus II	Right	12	-82	-38	216	7.05	<.001
LOC / MTG	Left	-41	-76	-10	761	6.82	<.001
IFG *pt* / IFG *po*	Left	-50	34	11	171	6.36	<.001
LOC / Occ P	Right	46	-73	-8	489	6.22	<.001
PHG / TFc / ITG	Left	-29	-30	-21	300	6.18	<.001
Cerebellum Vermis IX	Left	-2	-55	-35	118	4.67	.002
Association > Control							
PHG / LOC / TFc	Left	-31	-30	-19	2841	9.56	<.001
Cerebellum Crus II	Right	12	-82	-38	307	7.27	<.001
TFc / TOFc / LOC	Right	40	-25	-19	1515	7.25	<.001
Cerebellum IX	Right	10	-46	-49	248	6.87	<.001
Temporal P	Left	-43	14	-31	75	5.94	.026
Temporal P	Right	44	16	-24	78	5.78	.021
FOc	Left	-36	34	-12	92	5.67	.009
IFG *po*	Left	-41	18	22	110	4.85	.003
MTG /STG	Left	-54	-5	-19	103	4.82	.005

All results are thresholded at $p < .05$ (FWE, cluster level)
Brain region labels are given according the Harvard-Oxford Cortical and Subcortical Structural Atlas
IFG *pt* : inferior frontal gyrus pars triangularis; FG: fusiform gyrus; SMG: supramarginal gyrus; TOFc: temporo-occipital fusiform cortex; PCG: paracingulate gyrus; SFG: superior frontal gyrus; LOC: lateral occipital cortex; MTG: middle temporal gyrus;
IFG *po* : inferior frontal gyrus pars opercularis; Occ P: Occipital Pole; PHG: parahippocampal gyrus; TFc: temporal fusiform cortex; ITG: inferior temporal gyrus; OccFG: occipital fusiform gyrus; Temporal P: temporal poleFOc: frontal orbital cortex

Second, we entered the individual maps of parameters estimates for the three conditions (Manipulation, Function, Association) in a repeated-measure ANOVA with Task as within-subject factor. As shown in **Figure 4** and **Table 3**, the ANOVA revealed several regions that distinguished between the three conditions, that is, left SMG/IPS, left LOTC, and bilateral AG. The post-hoc ROI analysis centered on left LOTC cluster (MNI: -47,-62,-8; extent = 111 voxels) showed that Manipulation (*mean* β = 2.24, *SE* = .16) elicited greater activation than Function (*mean* β = 1.53, *SE* = .13, $t(34) = 9.85$, $p < .001$) and Association (*mean* β = 1.25, *SE* = .12, $t(34) = 8.44$, $p < .001$), Function elicited greater activation than Association ($t(34) = 3.18$, $p = .003$). The same pattern of result was found in left SMG/IPS cluster (MNI: -57,-30,36; extent = 787 voxels), Manipulation (*mean* β = 1.50, *SE* = .13) elicited greater activations than Function (*mean* β = .59, *SE* = .11, $t(34) = 10.13$, $p < .001$) and Association

(*mean* β = .43, *SE* = .07, *t*(34) = 10.46, *p* < .001), and Function yield to greater activations than Association (*t*(34) = 2.13, *p* = .041). In bilateral AG clusters (left: MNI: -43,-66,22; extent = 819 voxels; right: MNI: 51,-64,15; extent = 1016 voxels), Association (left: *mean* β = .49, *SE* = .09; right: *mean* β = .56, *SE* = .07) elicited greater changes in neural activity than Manipulation (left: *mean* β = -.32, *SE* = .09, *t*(34) = -8.01, *p* < .001; right: *mean* β = -.28, *SE* = .09, *t*(34) = -9.27, *p* < .001) and Function (left: *mean* β = -.33, *SE* = .06, *t*(34) = -10.89, *p* < .001; right: *mean* β = -.21, *SE* = .07, *t*(34) = -10.15, *p* < .001), whereas there were no differences between Manipulation and Function conditions (all *ts* < 1). Additionally, we observed a greater change in neural activity in the Association condition compared to the two other conditions in bilateral parahippocampal gyri (PHG) (see **Supplementary Figure 2**).

The same *post-hoc* analysis was conducted in each spherical ROI (see **Supplementary Figure 3**). Taken together, these results showed a superiority for the Manipulation condition in the ventro-dorsal pathway (SMG/IPS) as well as in the lateral part of the LOTC (from pMTG to pFG). The inferior part of the LOTC (mFG) showed similar brain activity for the three conditions. The lateral part of the LOTC may be more sensitive to Function compared to Association whereas the superior part of the LOTC (pMTG/AG) showed the opposite pattern.

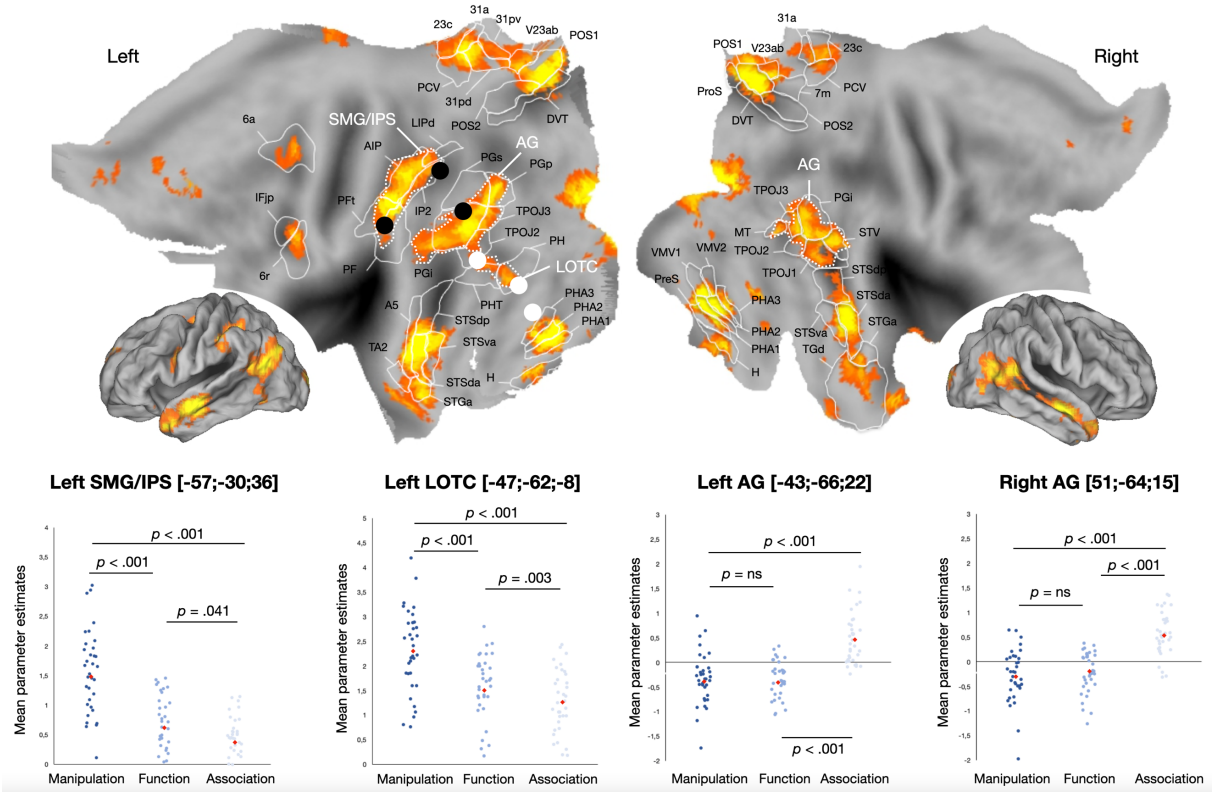

Figure 4. Brain regions showing a main effect of the factor Task in the one-way repeated measure ANOVA. Statistical maps for the main effect of task, as well as the 6 ROIs of the posterior TPN (ventral pathway = white; ventro-dorsal = black) are projected on PALS-B12 atlas surface configurations (Van Essen 2005) and are FWE-corrected ($p < .01$) for multiple comparisons across the whole-brain at the voxel level using an extent threshold of 50 voxels. The parcellation is based on Glasser et al. (2016). For the abbreviations, see Appendix (top). ROI analysis with parameter estimates for Manipulation, Function and Association was calculated within each brain region of interest that showed a significant effect in the ANOVA (i.e., SMG/IPS, LOTC and AG). Means for each condition are represented with a red diamond. ns: non-significant (bottom). LOTC: lateral occipitotemporal cortex; SMG/IPS: supramarginal gyrus/intraparietal sulcus; AG: angular gyrus.

Table 3. Regions activated in one-way repeated-measure ANOVA

Brain region	Hemisphere	Peak MNI coordinates			Cluster size	F-value	P_{FWE}
		x	y	z			
PHG	Right	24	-34	-15	758	98.77	<.001
Precuneus	Right	21	-57	20	1617	73.75	<.001
MTG	Left	-54	-5	-19	764	72.22	<.001
Lingual G/TOFc	Left	-24	-46	-8	276	71.54	<.001
Occ P	Right	17	-99	11	334	56.26	<.001
SMG	Left	-57	-30	36	787	56.08	<.001
Occ P	Left	-11	-101	2	255	53.75	<.001
STG/MTG	Right	51	-7	-17	333	53.38	<.001
LOC/AG	Left	-43	-66	22	819	52.72	<.001
LOC/AG	Right	51	-64	15	1016	42.19	<.001
PHG	Left	-20	-14	-24	154	40.27	<.001
IFG *po*	Left	-47	7	22	177	39.83	<.001
LOC/ITG/MTG	Left	-47	-62	-8	111	34.52	<.001
SFG	Left	-24	-9	54	62	31.82	<.001
SFG/Frontal P	Left	-8	57	34	80	29.82	<.001
FMC/PCG	Left	-2	43	-15	87	26.13	<.001

All results are thresholded at $p < .01$ (FWE, voxel level)
Brain region labels are given according the Harvard-Oxford Cortical and Subcortical Structural Atlas
PHG: parahippocampal gyrus; MTG: middle temporal gyrus; Lingual G: Lingual Gyrus; TOFc: temporal occipital fusiform cortex; Occ P: Occipital Pole; SMG: supramarginal gyrus; STG: superior temporal gyrus; LOC: lateral occipital cortex; AG: Angular Gyrus; IFG *po* : inferior; frontal gyrus pars opercularis; ITG: inferior temporal gyrus; SFG: superior frontal gyrus; Frontal P: frontal pole; FMC: frontal medial cortex; PCG: paracingulate gyrus

Finally, the conjunction analysis showed the commonalities between the three conditions. Similar neural activity was found in bilateral inferior lateral and ventral occipito-temporal cortices, bilateral posterior IPS, bilateral precentral gyrus, bilateral IFG (*pars opercularis*) and right middle frontal gyrus (see **Supplementary Figure 4** and **Supplementary Table 4**).

3.3. Functional connectivity analyses

The modulation of functional connectivity according to Manipulation, Function and Association tasks versus control tasks is represented in **Figure 5**. We observed significant modulations of functional connectivity for Manipulation, Function and Association compared to control conditions in the posterior TPN. Contrasts between tasks also led to significant modulation in functional connectivity in posterior TPN. We also contrasted control conditions against each other (Control_OC > Control_OO and Control_OO >Control_OC), but no difference in functional connectivity was observed.

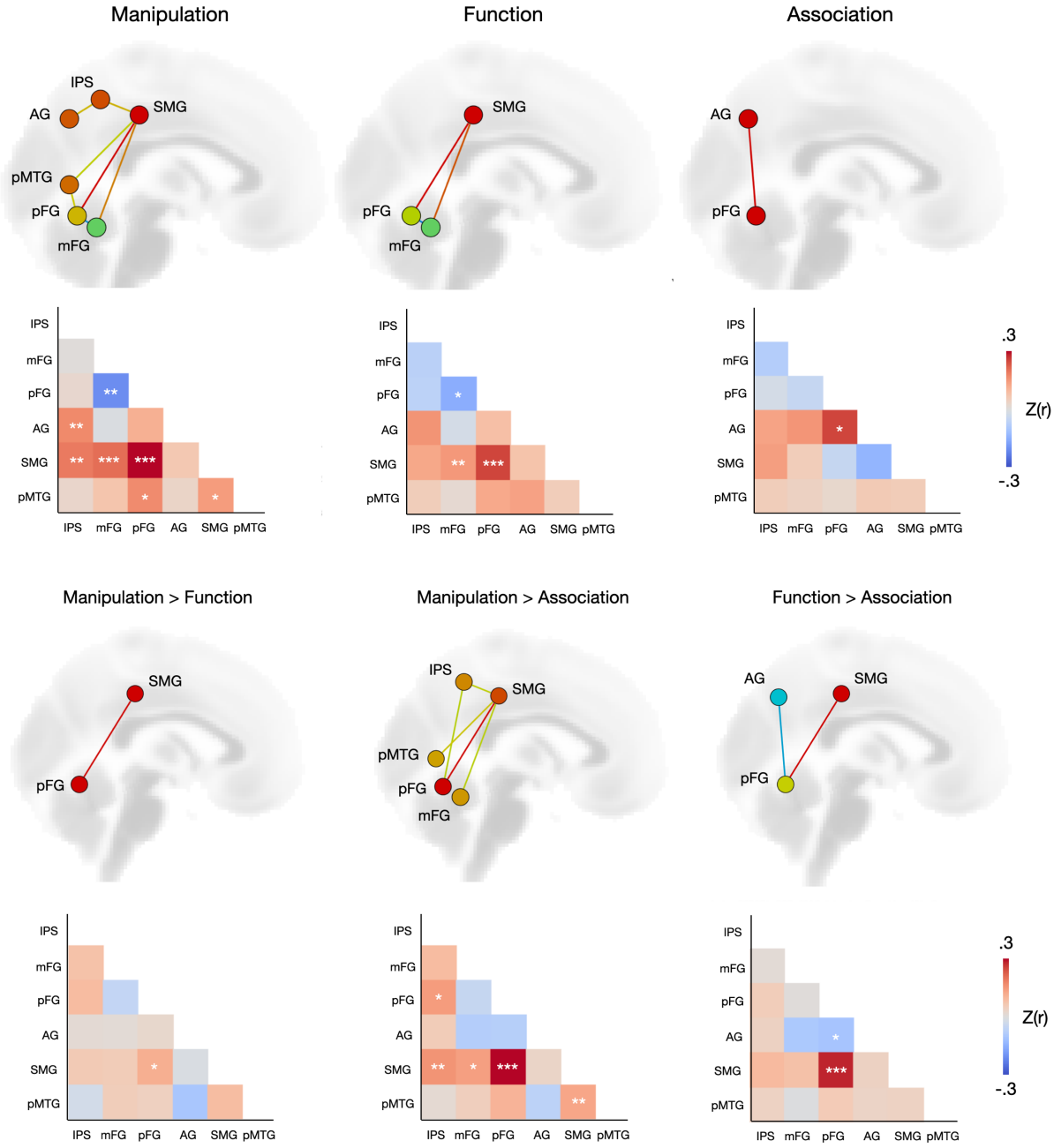

Figure 5. Functional connectivity within the 6 seed ROIs for Manipulation *vs* Control, Function *vs* Control and Association *vs* Control (top), and Manipulation *vs* Function, Manipulation *vs* Association, and Function *vs* Association (bottom). Sagittal view of the ROI-to-ROI functional connectivity (*p*-FDR seed-level corrected < .05) and pairwise correlation matrices (Z-Fisher transformed) are used to visualize both significant and non-significant correlations at *p*-FDR seed-level corrected < .05 (see **Supplementary Table 5 A-F** for pairwise correlation values). The color of ROIs in sagittal plots corresponds to the number of positive/negative connections to/from each ROI (summing the number of positive connections and subtracting the number of negative connections), so red indicates mostly positive connections to/from an ROI, and blue indicates mostly negative connections. The color of edges is varying from negative connectivity values (dark blue) to positive connectivity values (dark red). *** $p < .001$, ** $p < .01$, * $p < .05$, (*p*-FDR seed-level corrected).

First, we found that the number of edges that survived FDR-corrected alpha levels was the most important for Manipulation (n = 14, allowing duplicated counts from both sides; see **Table 4**), followed by Function (n = 6) and Association (n = 2) tasks. Second, an examination of the pattern of functional connectivity revealed that each condition was associated with the coupling of ventro-dorsal and ventral pathways, but each pattern was task-specific. In Manipulation task, the left SMG was associated with an increase of functional connectivity with IPS, $t(34) = 3.24$, $p < .01$, with LOTC (pMTG, $t(34) = 2.58$, $p < .05$ and pFG, $t(34) = 7.47$, $p < .001$) and with inferior LOTC (mFG, $t(34) = 4.45$, $p < .001$). In the function task, the left SMG exhibited an increase of functional connectivity with lateral and ventral structures of the occipitotemporal cortex (pFG, $t(34) = 4.57$, $p < .001$ and mFG, $t(34) = 3.36$, $p < .01$), but with no other parietal structures. In Association task, the left AG was associated with an increase of functional connectivity with pFG, $t(34) = 3.31$, $p < .01$.

Table 4. ROI-to-ROI Functional Connectivity for Manipulation, Function and Association. F-test values, Functional Connectivity intensity and number of ROIs showing significant Functional Connectivity with each ROI at p-FDR seed-level corrected < .05, ordered by F-values strength.

Manipulation				Function				Association			
ROI	F(5,30)	FC Intensity	Number	ROI	F(5,30)	FC Intensity	Number		F(5,30)	FC Intensity	Number
pFG	20.86	13.92	3	pFG	7.70	7.23	2	AG	3.15	3.31	1
SMG	11.98	17.40	4	SMG	6.27	7.94	2	pFG	2.05	3.31	1
mFG	6.10	8.32	2	mFG	4.65	6.01	2				
IPS	4.39	6.31	2								
pMTG	3.19	4.82	2								
AG	2.92	3.07	1								

When considering the difference between tasks, we found distinct functional connectivity patterns (see **Figure 5**). Difference between Manipulation and Function tasks led to an increase of functional connectivity between SMG and pFG, $t(34) = 2.84$, $p < .05$. This increase of functional connectivity between SMG and pFG was also present when factoring out the control task (see **Supplementary Table 6**). Difference between Manipulation and Association task was associated with an increase of functional connectivity between SMG-pFG, $t(34) = 10.09$, $p < .001$, SMG-pMTG, $t(34) = 3.67$, $p < .01$, SMG-IPS, $t(34) = 2.96$, $p < .01$, SMG-mFG, $t(34) = 2.75$, $p < .05$, and IPS-pFG, $t(34) = 2.70$, $p < .05$. Finally the contrast between Function and

Association tasks revealed an increase of functional connectivity between SMG-pFG, $t(34) = 5.77$, $p < .001$ and a decrease of FC between pFG-AG, $t(34) = -2.73$, $p < .05$.

4. Discussion

In the traditional neurocognitive account of action tool and semantic tool knowledge, action tool knowledge is considered to be mainly supported by ventro-dorsal pathway and semantic tool knowledge by the ventral pathway (e.g., Binkofski & Buxbaum, 2013). Several studies have investigated the neural bases of action tool and semantic tool tasks but no studies have considered function, association and manipulation tasks in the same experiment (see Lesourd et al., 2021). There were three main findings: (1) ventro-dorsal and ventral pathways are involved in both semantic tool and action tool knowledge, with semantic tool tasks engaging AG, PHG, LOTC and temporal pole whereas action tool tasks engaging SMG/IPS, LOTC and frontal regions; (2) function and association relations partly dissociate, with PHG and AG being more sensitive to association compared to function relations; (3) brain regions located in posterior TPN showed distinct patterns of functional connectivity as regards the nature of action tool and semantic tool relations, with an increase of functional connectivity between SMG and inferior LOTC during manipulation and function tasks and an increase of functional connectivity between AG and inferior LOTC during association task. These results will now be discussed in turn.

4.1. Ventral and ventro-dorsal pathways both contribute to action tool and semantic tool knowledge

We found that action tool knowledge was supported mainly by a left-lateralized network (Ishibashi et al., 2018; Ishibashi, Pobric, Saito, & Lambon Ralph, 2016; Reynaud et al., 2016). We showed that action tool knowledge relies mainly upon the left SMG/IPS and

additional frontal regions. This result is in agreement with previous fMRI studies which reported a specificity for action tool tasks compared to semantic tool tasks in the ventro-dorsal pathway (Boronat et al. 2005; Canessa et al. 2008; Kleineberg et al. 2018). Moreover, there is a large amount of literature on apraxia which reported that left brain damaged patients are impaired in manipulation tasks following lesions in left IPL (Buxbaum et al., 2007, 2014; Kalénine et al., 2010; Martin et al., 2017). The left SMG/IPS are associated with the ability to produce or to plan functional grasp (Reynaud et al. 2016; Przybylski and Króliczak 2017; Potok et al. 2019). We also found that the left LOTC was more sensitive to manipulation task compared to semantic tool tasks. The LOTC is known to play a role in the perception of object-related actions (Wurm, Caramazza, & Lingnau, 2017), the conceptual processing of tools and actions (Kable & Chatterjee, 2006; Lingnau & Downing, 2015; Wurm & Caramazza, 2019), and tool naming (Brambati et al., 2006).

LOTC also includes hand-selective representations that closely overlap with regions activated by tools (Bracci, Cavina-Pratesi, Ietswaart, Caramazza, & Peelen, 2012), suggesting that hand and object representations are tightly integrated (see 2AS+ model; Buxbaum, 2017). Neuropsychological studies found in LBD patients that a damage in left IPL is associated with a hand posture deficit and a damage in left pMTG is rather associated with kinematics deficit (Martin et al., 2017; see Buxbaum et al., 2014 for opposite results). In the present study, although participants were instructed to focus only on kinematics components of tools, we reported activations in left LOTC and left IPL. In fMRI studies, hand posture and kinematics components indifferently engage either IPL/IPS or pMTG (e.g., Kleineberg et al., 2018). However, stimulation studies showed that hand posture is impaired following virtual lesions in IPL (SMG) (Andres et al., 2013; Pelgrims et al., 2011), and kinematics-related knowledge is modulated following virtual lesions of inferior LOTC (Perini et al., 2014). These results suggest that kinematics are preferentially processed in the inferior LOTC, whereas hand posture is preferentially processed in the IPL (SMG). It is likely that when healthy

participants access to the kinematics of tool actions, they implicitly process the hand posture component. In broad terms, if hand posture and kinematics are two distinct representations (Lesourd, Naëgelé, Jaillard, Detante, & Osiurak, 2020; Sirigu, Cohen, Duhamep, Pillon, & Agid, 1995), they are mutually interacting with each other even when participants are asked to focus only on one dimension. This hypothesis could explain the pattern of results obtained in fMRI studies. Further studies are needed to unravel the precise contribution of IPL and LOTC for processing the components of action tool knowledge.

Semantic tool knowledge was found to activate bilateral AG. However, if ROI analyses showed that neural activity was higher in AG for association relations compared to function and manipulation relations, this brain activity was not significantly distinct from baseline. Previous fMRI studies showed that bilateral AG were more activated for association relations compared to manipulation relations (Kleineberg et al. 2018). The role of AG in semantic knowledge retrieval has already been reported (Binder, Desai, Graves, & Conant, 2009), more specifically in thematic or combinatorial processing (Binder & Desai, 2011; Price, Bonner, Peelle, & Grossman, 2015). We also reported the involvement of PHG and retrosplenial cortex. Previous fMRI and PET studies showed that PHG and retrosplenial cortex are both engaged in processing contextual associations and in scene selectivity (Nakamura 2000; Bar and Aminoff 2003; Aminoff et al. 2007; Canessa et al. 2008; Hutchison et al. 2014; Chen et al. 2016; Hutchison and Gallivan 2018). In our association task, participants had to judge whether a tool (e.g., screwdriver) can be found in a given context (e.g., desk). This can explain why we found activations in bilateral AG and additional selective visual scene areas, compared to other association tasks where only a tool and an object are displayed (e.g., hammer and nail; Kleineberg et al., 2018).

Finally, our findings indicate that both action tool and semantic tool knowledge activate posterior inferior occipito-temporal cortices. Previous studies found that judgement about the context of use and judgement about the manipulation both activate inferior LOTC, posterior

IPS, pMTG and IFG (Canessa et al. 2008), suggesting that action tool and semantic tool representations may rely in part on common brain regions.

4.2. Functional coupling within the posterior TPN during the retrieval of action tool and semantic tool knowledge

Our results revealed that both action tool and semantic tool knowledge was associated with the coupling between posterior regions of the TPN. Importantly, action tool and semantic tool representations elicited distinct functional connectivity patterns, that is, an increase of functional connectivity between SMG and fusiform gyrii (pFG and mFG) for manipulation and function relations and an increase of functional connectivity between AG and posterior fusiform gyrus (pFG) for association relations. Thus, the explicit retrieval of tool knowledge may require the integration of specific tool features which are stored or processed in dedicated regions of the TPN (see for example Mahon & Caramazza, 2011).

Manipulation relations involved a wider network than function relations, comprising parietal (AG and IPS) and temporal (pMTG) regions. We also showed that the strength of the association between IPL/SMG and ventral LOTC (pFG) was higher for manipulation than for function relations. This corroborates the idea that function relations rather call upon ventral LOTC, whereas manipulation relations are supported by several regions in LOTC and IPL (Buxbaum et al., 2014; Kalénine & Buxbaum, 2016; Kalénine et al., 2010; Martin et al., 2017; Tarhan et al., 2015). We also reported an increase of functional connectivity between pMTG and SMG only for manipulation relations. pMTG is at the edge of regions which process body parts and tools (Lingnau and Downing 2015) and it is therefore likely that manipulation relations are supported by brain regions in which hands and tools are tightly integrated (Bracci et al. 2012). It has been already showed that passively viewing images of manipulable tools is associated with an increase of connectivity between pMTG and IPL (Garcea et al.,

2018). Other studies also pointed out the structural connectivity existing between IPL and pMTG (Caspers et al., 2011; Vry et al., 2015). Moreover, the production of pantomime of tool use, which requires the activation of action tool knowledge (Buxbaum, 2014; Buxbaum et al., 2007, 2005; Lesourd et al., 2019), is associated with an increase of functional connectivity between the left inferior LOTC and the left IPL (Vingerhoets and Clauwaert 2015; Garcea et al. 2018).

These data suggested that action tool and semantic tool knowledge may be retrieved by the way of mutual exchange between the ventral and the dorso-ventral pathways. Moreover, both LOTC and IPL represent key regions in ventral and dorso-ventral pathways, respectively.

4.3. Neurocognitive processes supported by the posterior TPN

4.3.1. Function and association judgment tasks, two sides of the same coin?

Our results suggest that some structures are more engaged in association relations than in function relations. Neural activity was stronger in PHG and AG in association relations compared to function relations. Previous studies found that AG and PHG were more involved in association relations compared to manipulation relations (Canessa et al. 2008; Kleineberg et al. 2018). PHG was also found to be more involved in function compared to manipulation (Chen et al. 2016), but to our knowledge no studies have directly contrasted function and association judgment tasks. Taken together these data indicate that PHG may be more sensitive to scene or contextual information included in association judgment compared to function judgment. We also reported that function relations elicited more activations in LOTC compared to association relations. LOTC is known to store abstract representations about actions, and particularly its ventral part, for transitive actions (Wurm et al. 2017). These results acknowledge the links between function and manipulation representations, by showing

that the LOTC, which is tuned for action representation, is also engaged in the processing of function relations. We also found a marginal difference between function and association with SMG/IPS, but neither function nor association against control conditions revealed significant activations in SMG/IPS in whole brain analysis. These data are in agreement with stimulations studies which did not find direct effect of virtual lesion in SMG/IPS for function and association judgement tasks (Ishibashi et al. 2011, 2018; Andres et al. 2013). Moreover, association did not elicit any activations compared to manipulation tasks in IPL(SMG) and IPS (Boronat et al. 2005; Canessa et al. 2008; Kleineberg et al. 2018). Our data suggest that function and association judgment tasks may be represented, at least in part, by distinct brain regions. Support for this also comes from a recent work, in which we also found neuropsychological dissociations in LBD patients' studies (i.e., 29-47%; percentage varying according to the studies), suggesting that these relations are also supported by distinct cognitive systems (for a review see Lesourd et al., 2021).

4.3.2. Function and manipulation judgment task rely upon distinct but interacting brain regions

There has been a long debate in the literature about the potential link between function and manipulation knowledge, and particularly the involvement of the left IPL in function relations. Neuropsychological dissociations have been reported (Buxbaum & Saffran, 2002; Garcea, Dombovy, & Mahon, 2013; Sirigu, Duhamel, & Poncet, 1991) and studies on healthy participants also revealed that function and manipulation knowledge can be accessed independently from each other (Garcea and Mahon 2012). Recent neuroimaging studies reported that function and manipulation are supported by distinct brain regions, that is, IPL for manipulation and medial fusiform gyrus for function knowledge (Chen et al. 2016, 2018). Some stimulation studies reported that neither association nor function judgment tasks are

impacted following virtual lesions made either in IPS or SMG (Ishibashi et al. 2011, 2018; Andres et al. 2013). In the present study we found that both function and manipulation judgment tasks were associated with activations in inferior LOTC and fusiform gyrus, but only manipulation judgment task engaged parietal structures. This result is in line with the abovementioned literature.

However, we found an increase of functional connectivity between the left SMG and the left fusiform gyrus in both function and manipulation tasks. The left IPL is assumed to represent abstract knowledge about action but not function (Chen et al. 2016, 2018), however, its precise role in function relation is under debate. For instance, a recent stimulation study showed in a priming task that function judgement, but not association, can be impaired following virtual lesion made in pMTG and at a lesser extent in SMG, during the presentation of a related manipulative prime (De Bellis et al. 2020). This latter result highlighted the links between manipulation and function representations, but it also pointed out that both left pMTG and left IPL preferentially mediate the effect of manipulation representation on function judgement task rather than being the store of function representations. In a fMRI-adaptation paradigm, Yee et al. (2010) found that adaptation in left IPS was predicted by the degree of function similarity between word pairs and was also predicted by the degree of manipulation similarity. However, as manipulation and function similarity were highly correlated together and function condition did not elicit any activation in this region in whole brain analysis, it is therefore likely that manipulation accounts for this relationship.

Taken together, these data suggest that the left SMG/IPS does not store representations neither about function relations nor on association relations (Ishibashi et al. 2011, 2018; Andres et al. 2013) but the explicit retrieval of knowledge about function relations may require the coupling between abstract nodes of the posterior TPN.

4.4. Implication for theories of tool use

The role of the left IPL in action tool knowledge is a matter of debate between two current neurocognitive accounts of tool use. According to the manipulation-based approach (Buxbaum, 2017), the ventro-dorsal pathway, particularly the left IPL, stores manipulation knowledge which contains canonical learned actions abstracted over experience. Manipulation knowledge focuses on hand-tool relations (i.e., egocentric relationships) and is assumed to support mainly familiar use of tools. According to the reasoning-based approach (Osiurak et al., 2020), the left IPL, more particularly the area PF in SMG, is more likely to contain mechanical knowledge, a nondeclarative knowledge about physical principles that is acquired through experience. Mechanical knowledge focuses on tool-object relations (i.e., allocentric relationships) and is assumed to support both familiar and unfamiliar use of tools.

These two approaches make distinct predictions concerning the involvement of the left IPL in manipulation judgment tasks, as the one used in the present study. Manipulation judgment tasks focus on hand-tool relations (e.g., choosing the correct hand posture to grasp a given tool); thus, the left IPL should be particularly engaged in these tasks according to the manipulation-based approach. In contrast, according to the reasoning-based approach, the left SMG/PF, which is involved in allocentric relationships (i.e., tool-object) should not be engaged in manipulation judgment tasks. Our results indicated that the left SMG/PFt was engaged in the manipulation judgment task, suggesting, in agreement with the manipulation-based approach, that this brain area may store manipulation knowledge. However, this brain region is also considered as a regional hub, integrating representations from several nodes (Orban and Caruana 2014; Reynaud et al. 2016, 2019) and may not contain sensory-motor knowledge.

In agreement with the reasoning-based approach, PF was not activated in the manipulation judgement task in univariate contrasts, suggesting that this region is not

sensitive to egocentric relationships. However, we found that PF was involved in the brain network supporting the manipulation condition in the functional connectivity analyses. To explain this discrepancy, we propose two explanations. First, the coordinates of PF used in the functional connectivity analyses are at the edge of the area PF and PFt, which are both subregions of the SMG. Thus, the spherical SMG ROI built from PF coordinates may have also encompassed a part of PFt which is largely involved in the manipulation condition. Consequently, our SMG ROI has captured a part of variance from PFt. Second, it may suggest that PF is involved in egocentric relationships and not only in allocentric ones, which may contradict a key prediction from the reasoning-based approach. Further studies are required to disentangle the role of PF in manipulation judgement tasks.

4.5. Limitations

We found in the pretest that the three conditions were not equivalent in terms of difficulty, i.e., manipulation condition was harder than function condition, which was in turn harder than association condition. One may assume that our results may be explained by variations in task difficulty rather than by the nature of the neurocognitive processes involved in these tasks (see Kleineberg et al., 2018 for a similar discussion). In LBD patients' studies, if control participants succeed equally in terms of accuracy for manipulation and function tasks, association tasks appear easier (Bartolo, Daumüller, Della Sala, & Goldenberg, 2007; Lesourd et al., 2019). However, when difficulty is equally maintained across conditions (i.e., accuracy), Kalénine and Buxbaum, (2016) found that both left brain-damaged patients and control participants were slower to identify function than association relationships. A similar result was found in healthy participants between manipulation and function matching tasks, where reaction times in the manipulation condition were slower than in the function condition, after controlling for task difficulty (Canessa et al. 2008; Garcea and Mahon 2012).

Moreover, our results are in general agreement with other fMRI studies which have reported similar accuracies across conditions and greater activations in IPL/IPS for action tool compared to semantic tool tasks (Canessa et al. 2008; Kleineberg et al. 2018). In summary, action tool tasks as regards to semantic tool tasks are characterized by (1) slower judgement reaction times or lower accuracies; and (2) greater brain activation in IPL/IPS. These findings go against the task complexity hypothesis.

We also found that the control condition for Manipulation and Function conditions was weaker than the control condition for Association condition in the univariate analysis, resulting in bilateral activation of bilateral LOTC. This observation could explain why we found a weaker involvement of the left pMTG, which is a part of the LOTC (Lingnau & Downing, 2015), in the Association condition, whereas this brain region is known to be involved in thematic and contextual/association relations (Andres et al. 2013; Kalénine and Buxbaum 2016; Lesourd et al. 2021). Although there was no difference between the brain networks associated with the two control conditions in the functional analysis, it is likely that contrasting the Association condition with its control condition was sufficient to decrease the involvement of the left pMTG.

5. Conclusions

It is traditionally assumed that action tool and semantic tool knowledge are supported by the ventro-dorsal and the ventral pathways, respectively. Our data confirm overall this functional organization but provide further details, by showing that, AG in the ventro-dorsal pathway is sensitive to association relations whereas LOTC in the ventral pathways is rather sensitive to manipulation and function relations. Moreover, we observed specific modulation in functional connectivity in the posterior TPN during action tool and semantic tool tasks, depending on the kind of relation. Retrieval of manipulation and function knowledge is associated with the coupling between SMG and FG, whereas association knowledge is

supported by the coupling between AG and FG. Altogether, these data suggest that the explicit retrieval of tool knowledge is supported by the functional coupling between brain regions in the posterior TPN, each processing specific tool features.

Further studies are now warranted to characterize the precise contribution of each posterior TPN region in specific feature of tool knowledge, particularly for action tool knowledge (i.e., hand posture and kinematics), by using lesion symptom mapping in brain damaged patients and MVPA in healthy participants.

Appendix

Abbreviations of cerebral areas based on the Multi-modal parcellation of human cerebral cortex (Glasser et al. 2016)

MT+ complex and neighboring visual areas	FST	Area FST
	PH	Area PH
	LO2	Area Lateral Occipital 2
	MT	Middle Temporal Area
	MST	Medial Superior Temporal Area
	V4t	Area V4t
Lateral temporal cortex	PHT	Aera PHT
	TE2p	Area TE2 posterior
	TF	Aera TF
Ventral stream visual cortex	FFC	Fusiform Face Complex
	PHA1	ParaHippocampal Area 1
	PHA2	ParaHippocampal Area 2
	PHA3	ParaHippocampal Area 3
	PIT	Posterior InferoTemporal
Temporo-Parieto-Occipital Junction	TPOJ1	Area Temporo-parieto-occipital junction 1
	TPOJ2	Area Temporo-parieto-occipital junction 2
	TPOJ3	Area Temporo-parieto-occipital junction 2
Inferior parietal cortex	PGi	Area PGi (Angular Gyrus)
	PGs	Area PGs (Angular Gyrus)
	PGp	Area PGp (Supramarginal gyrus)
	PF	Area PF (Supramarginal gyrus)
	PFt	Area PFt (Supramarginal gyrus)
	IP0	Area intraparietal 0
	IP2	Area intraparietal 2
Superior parietal cortex	AIP	Anterior Intraparietal Area
	LIPd	Area Lateral Intraparietal dorsal
Medial Temporal Cortex	H	Hippocampus
	PreS	Presubiculum
	VM 1-2	Ventromedial visual areas 1-2
Dorsal Stream Visual cortex	IPS1	IntraParietal Sulcus Area 1
	V7	Seventh Visual Area
	V3B	Area V3B
	DVT	Dorsal Visual Transitional Area
Posterior cingulate cortex	31pd	Area 31pd
	7m	Area 7m
	POS1	Parieto-Occipital Sulcus Area 1
	POS2	Parieto-Occipital Sulcus Area 2
	v23ab	Area ventral 23 a+b
	PCV	Posterior Cingulate Visual Area
	23c	Area 23c
	31a	Area 31a
	31pv	Area 31p ventral
	ProS	ProStriate Area
Anterior cingulate and medial prefrontal cortex	8BM	Area 8BM
	p32pr	Area p32 prime
Premotor cortex	6r	Rostral area 6 – inferior premotor
	6a	Area 6 anterior – superior premotor
Insular and Frontal Opercular Cortex	AAIC	Anterior Agranular Insula Complex
	AVI	Anterior Ventral Insular Area
Inferior Frontal Cortex	44	Area 44
	45	Area 45
	IFSp	Area IFSp
	IFJa	Area IFJa
	IFJp	Area IFJp
Auditory Association Cortex	TA2	Area TA2
	A5	Auditory 5 Complex
	STSdp	Area STSd posterior
	STSva	Area STSv anterior
	STSda	Area STSd anterior
	STGa	Area STGa

Acknowledgments

This work was supported by Agence Nationale de la Recherche Grant ANR-14-CE30-0015-01ANR and was performed within the framework of the LABEX CORTEX (ANR-11LABX-0042) of the Université de Lyon within the program “Investissements d’Avenir” (ANR-11-IDEX-0007) operated by the French National Research Agency. This work was also supported by grants from Region Bourgogne Franche-Comté (“REPRESACT” Project, AAP Amorçage 2021) and University of Franche-Comté (AAP Chrysalide 2020-2021).

We warmly thank Emmanuel de Oliveira for his help in preparing the stimuli and collecting the data.

Data and Code availability statement

Unthresholded statistical maps for the main contrasts of interest can be visualized on NeuroVault (https://neurovault.org/collections/10011/). Stimulus materials and code are available upon reasonable request.

References

Almeida J, Fintzi AR, Mahon BZ. 2013. Tool manipulation knowledge is retrieved by way of the ventral visual object processing pathway. Cortex. 49:2334–2344.

Ambrose SH. 2001. Paleolithic Technology and Human Evolution. Science (80-). 291:1748–1753.

Aminoff E, Gronau N, Bar M. 2007. The Parahippocampal Cortex Mediates Spatial and Nonspatial Associations. Cereb Cortex. 17:1493–1503.

Andersson JLR, Skare S, Ashburner J. 2003. How to correct susceptibility distortions in spin-echo echo-planar images: application to diffusion tensor imaging. Neuroimage. 20:870–888.

Andres M, Pelgrims B, Olivier E. 2013. Distinct contribution of the parietal and temporal cortex to hand configuration and contextual judgements about tools. Cortex. 49:2097–2105.

Bar M, Aminoff E. 2003. Cortical Analysis of Visual Context. Neuron. 38:347–358.

Bartolo A, Daumüller M, Della Sala S, Goldenberg G. 2007. Relationship between Object-Related Gestures and the Fractionated Object Knowledge System. Behav Neurol. 18:143–147.

Baumard J, Lesourd M, Jarry C, Merck C, Etcharry-Bouyx F, Chauviré V, Belliard S, Moreaud O, Croisile B, Osiurak F, Le Gall D. 2016. Tool use disorders in neurodegenerative diseases: Roles of semantic memory and technical reasoning. Cortex. 82:119–132.

Baumard J, Lesourd M, Remigereau C, Merck C, Jarry C, Etcharry-Bouyx F, Chauviré V, Belliard S, Moreaud O, Osiurak F, Le Gall D. 2019. The – weak – role of memory in tool use: Evidence from neurodegenerative diseases. Neuropsychologia. 129:117–132.

Behzadi Y, Restom K, Liau J, Liu TT. 2007. A component based noise correction method

(CompCor) for BOLD and perfusion based fMRI. Neuroimage. 37:90–101.

Binder JR, Desai RH, Graves WW, Conant LL. 2009. Where is the semantic system? A critical review and meta-analysis of 120 functional neuroimaging studies. Cereb Cortex. 19:2767–2796.

Binkofski F, Buxbaum LJ. 2013. Two action systems in the human brain. Brain Lang. 127:222–229.

Boronat CB, Buxbaum LJ, Coslett HB, Tang K, Saffran EM, Kimberg DY, Detre JA. 2005. Distinctions between manipulation and function knowledge of objects: Evidence from functional magnetic resonance imaging. Cogn Brain Res. 23:361–373.

Bozeat S, Lambon Ralph MA, Patterson K, Hodges JR. 2002. When objects lose their meaning: what happens to their use? Cogn Affect Behav Neurosci. 2:236–251.

Bracci S, Cavina-Pratesi C, Ietswaart M, Caramazza A, Peelen M V. 2012. Closely overlapping responses to tools and hands in left lateral occipitotemporal cortex. J Neurophysiol. 107:1443–1446.

Buxbaum LJ. 2001. Ideomotor apraxia: a call to action. Neurocase. 7:445–448.

Buxbaum LJ. 2014. Moving the gesture engram into the 21st century. Cortex. 57:286–289.

Buxbaum LJ. 2017. Learning, remembering, and predicting how to use tools: Distributed neurocognitive mechanisms: Comment on Osiurak and Badets (2016). Psychol Rev. 124:346–360.

Buxbaum LJ, Kyle K, Grossman M, Coslett HB. 2007. Left inferior parietal representations for skilled hand-object interactions: Evidence from stroke and corticobasal degeneration. Cortex. 43:411–423.

Buxbaum LJ, Kyle KM, Menon R. 2005. On beyond mirror neurons: Internal representations subserving imitation and recognition of skilled object-related actions in humans. Cogn Brain Res. 25:226–239.

Buxbaum LJ, Saffran EM. 2002. Knowledge of object manipulation and object function:

Dissociations in apraxic and nonapraxic subjects. Brain Lang. 82:179–199.

Buxbaum LJ, Schwartz MF, Carew TG. 1997. The Role of Semantic Memory in Object Use. Cogn Neuropsychol. 14:219–254.

Buxbaum LJ, Shapiro AD, Coslett HB. 2014a. Critical brain regions for tool-related and imitative actions: A componential analysis. Brain. 137:1971–1985.

Buxbaum LJ, Shapiro AD, Coslett HB. 2014b. Critical brain regions for tool-related and imitative actions: A componential analysis. Brain. 137:1971–1985.

Canessa N, Borgo F, Cappa SF, Perani D, Falini A, Buccino G, Tettamanti M, Shallice T. 2008. The different neural correlates of action and functional knowledge in semantic memory: An fMRI study. Cereb Cortex. 18:740–751.

Chen Q, Garcea FE, Jacobs RA, Mahon BZ. 2018. Abstract representations of object-directed action in the left inferior parietal lobule. Cereb Cortex. 28:2162–2174.

Chen Q, Garcea FE, Mahon BZ. 2016. The Representation of Object-Directed Action and Function Knowledge in the Human Brain. Cereb Cortex. 26:1609–1618.

De Bellis F, Magliacano A, Sagliano L, Conson M, Grossi D, Trojano L. 2020. Left inferior parietal and posterior temporal cortices mediate the effect of action observation on semantic processing of objects: evidence from rTMS. Psychol Res. 84:1006–1019.

Ebisch SJH, Babiloni C, Del Gratta C, Ferretti A, Perrucci MG, Caulo M, Sitskoorn MM, Romani GL. 2007. Human neural systems for conceptual knowledge of proper object use: A functional magnetic resonance imaging study. Cereb Cortex. 17:2744–2751.

Eickhoff SB, Stephan KE, Mohlberg H, Grefkes C, Fink GR, Amunts K, Zilles K. 2005. A new SPM toolbox for combining probabilistic cytoarchitectonic maps and functional imaging data. Neuroimage. 25:1325–1335.

Gallivan JP, Adam McLean D, Valyear KF, Culham JC. 2013. Decoding the neural mechanisms of human tool use. Elife. 2013:1–29.

Garcea FE, Chen Q, Vargas R, Narayan DA, Mahon BZ. 2018. Task- and domain-specific

modulation of functional connectivity in the ventral and dorsal object-processing pathways. Brain Struct Funct. 223:2589–2607.

Garcea FE, Dombovy M, Mahon BZ. 2013. Preserved tool knowledge in the context of impaired action knowledge: Implications for models of semantic memory. Front Hum Neurosci. 7:1–18.

Garcea FE, Mahon BZ. 2012. What is in a tool concept? Dissociating manipulation knowledge from function knowledge. Mem Cogn. 40:1303–1313.

Glasser MF, Coalson TS, Robinson EC, Hacker CD, Harwell J, Yacoub E, Ugurbil K, Andersson J, Beckmann CF, Jenkinson M, Smith SM, Van Essen DC. 2016. A multi-modal parcellation of human cerebral cortex. Nature. 536:171–178.

Goldenberg G. 2013. Apraxia. Oxford: Oxford University Press.

Goldenberg G, Randerath J. 2015. Shared neural substrates of apraxia and aphasia. Neuropsychologia. 75:40–49.

Goldenberg G, Spatt J. 2009. The neural basis of tool use. Brain. 132:1645–1655.

Goodale MA, Milner AD. 1992. Separate visual pathways for perception and action. Trends Neurosci. 15:20–25.

Hodges JR, Bozeat S, Lambon Ralph MA, Patterson K, Spatt J. 2000. The role of conceptual knowledge in object use: Evidence from semantic dementia. Brain. 123:1913–1925.

Hutchison RM, Culham JC, Everling S, Flanagan JR, Gallivan JP. 2014. Distinct and distributed functional connectivity patterns across cortex reflect the domain-specific constraints of object, face, scene, body, and tool category-selective modules in the ventral visual pathway. Neuroimage. 96:216–236.

Hutchison RM, Gallivan JP. 2018. Functional coupling between frontoparietal and occipitotemporal pathways during action and perception. Cortex. 98:8–27.

Ishibashi R, Lambon Ralph MA, Saito S, Pobric G. 2011. Different roles of lateral anterior temporal lobe and inferior parietal lobule in coding function and manipulation tool

knowledge: Evidence from an rTMS study. Neuropsychologia. 49:1128–1135.

Ishibashi R, Mima T, Fukuyama H, Pobric G. 2018. Facilitation of function and manipulation knowledge of tools using transcranial direct current stimulation (tDCS). Front Integr Neurosci. 11:1–8.

Ishibashi R, Pobric G, Saito S, Lambon Ralph MA. 2016. The neural network for tool-related cognition: An activation likelihood estimation meta-analysis of 49 neuroimaging studies. Cogn Neuropsychol. 33:241–256.

Johnson-Frey SH. 2004. The neural bases of complex tool use in humans. Trends Cogn Sci. 8:71–78.

Johnson-Frey SH, Newman-Norlund R, Grafton ST. 2005. A distributed left hemisphere network active during planning of everyday tool use skills. Cereb Cortex. 15:681–695.

Kalénine S, Buxbaum LJ. 2016. Thematic knowledge, artifact concepts, and the left posterior temporal lobe: Where action and object semantics converge. Cortex. 82:164–178.

Kalénine S, Buxbaum LJ, Coslett HB. 2010. Critical brain regions for action recognition: Lesion symptom mapping in left hemisphere stroke. Brain. 133:3269–3280.

Kellenbach ML, Brett M, Patterson K. 2003. Actions speak louder than functions: The importance of manipulability and action in tool representation. J Cogn Neurosci. 15:30–46.

Kleineberg NN, Dovern A, Binder E, Grefkes C, Eickhoff SB, Fink GR, Weiss PH. 2018. Action and semantic tool knowledge – Effective connectivity in the underlying neural networks. Hum Brain Mapp. 39:3473–3486.

Lacadie CM, Fulbright RK, Constable RT, Papademetris X. 2008. More accurate Talairach coordinates for neuroimaging using nonlinear registration. Neuroimage. 42:717–725.

Lesourd M, Baumard J, Jarry C, Etcharry-Bouyx F, Belliard S, Moreaud O, Croisile B, Chauviré V, Granjon M, Le Gall D, Osiurak F. 2017. Rethinking the Cognitive Mechanisms Underlying Pantomime of Tool Use: Evidence from Alzheimer's Disease

and Semantic Dementia. J Int Neuropsychol Soc. 23:128–138.

Lesourd M, Budriesi C, Osiurak F, Nichelli PF, Bartolo A. 2019. Mechanical knowledge does matter to tool use even when assessed with a non-production task: Evidence from left brain-damaged patients. J Neuropsychol. 13.

Lesourd M, Naëgelé B, Jaillard A, Detante O, Osiurak F. 2020. Using tools effectively despite defective hand posture: A single-case study. Cortex. 129:406–422.

Lesourd M, Servant M, Baumard J, Reynaud E, Ecochard C, Medjaoui FT, Bartolo A, Osiurak F. 2021. Semantic and action tool knowledge in the brain: Identifying common and distinct networks. Neuropsychologia. 159:107918.

Lewis JW. 2006. Cortical networks related to human use of tools. Neuroscientist. 12:211–231.

Lingnau A, Downing PE. 2015. The lateral occipitotemporal cortex in action. Trends Cogn Sci. 19:268–277.

Mahon BZ, Caramazza A. 2011. What drives the organization of object knowledge in the brain? Trends Cogn Sci. 15:97–103.

Mahon BZ, Kumar N, Almeida J. 2013. Spatial Frequency Tuning Reveals Interactions between the Dorsal and Ventral Visual Systems. J Cogn Neurosci. 25:862–871.

Martin M, Beume L, Kümmerer D, Schmidt CSM, Bormann T, Dressing A, Ludwig VM, Umarova RM, Mader I, Rijntjes M, Kaller CP, Weiller C. 2016. Differential roles of ventral and dorsal streams for conceptual and production-related components of tool use in acute stroke patients. Cereb Cortex. 26:3754–3771.

Martin M, Dressing A, Bormann T, Schmidt CSM, Kümmerer D, Beume L, Saur D, Mader I, Rijntjes M, Kaller CP, Weiller C. 2017. Componential network for the recognition of tool-associated actions: Evidence from voxel-based lesion-symptom mapping in acute stroke patients. Cereb Cortex. 27:4139–4152.

Milner AD. 2017. How do the two visual streams interact with each other? Exp Brain Res.

235:1297–1308.

Mirman D, Landrigan J-F, Britt AE. 2017. Taxonomic and thematic semantic systems. Psychol Bull. 143:499–520.

Nakamura K. 2000. Functional delineation of the human occipito-temporal areas related to face and scene processing: A PET study. Brain. 123:1903–1912.

Negri GA, Lunardelli A, Reverberi C, Gigli GL, Rumiati RI. 2007. Degraded semantic knowledge and accurate object use. Cortex. 43:376–388.

Niessen E, Fink GR, Weiss PH. 2014. Apraxia, pantomime and the parietal cortex. NeuroImage Clin. 5:42–52.

Orban GA, Caruana F. 2014. The neural basis of human tool use. Front Psychol. 5:1–12.

Osiurak F, Badets A. 2016. Tool use and affordance: Manipulation-based versus reasoning-based approaches. Psychol Rev. 123:534–568.

Osiurak F, Jarry C, Le Gall D. 2010. Grasping the affordances, understanding the reasoning: toward a dialectical theory of human tool use. Psychol Rev. 117:517–540.

Osiurak F, Jarry C, Le Gall D. 2011. Re-examining the gesture engram hypothesis. New perspectives on apraxia of tool use. Neuropsychologia. 49:299–312.

Osiurak F, Lesourd M, Navarro J, Reynaud E. 2020. Technition: When Tools Come Out of the Closet. Perspect Psychol Sci.

Pelgrims B, Olivier E, Andres M. 2011. Dissociation between manipulation and conceptual knowledge of object use in the supramarginalis gyrus. Hum Brain Mapp. 32:1802–1810.

Potok W, Maskiewicz A, Króliczak G, Marangon M. 2019. The temporal involvement of the left supramarginal gyrus in planning functional grasps: A neuronavigated TMS study. Cortex. 111:16–34.

Przybylski Ł, Króliczak G. 2017. Planning Functional Grasps of Simple Tools Invokes the Hand-independent Praxis Representation Network: An fMRI Study. J Int Neuropsychol Soc. 23:108–120.

Randerath J, Goldenberg G, Spijkers W, Li Y, Hermsdörfer J. 2010. Different left brain regions are essential for grasping a tool compared with its subsequent use. Neuroimage. 53:171–180.

Randerath J, Li Y, Goldenberg G, Hermsdörfer J. 2009. Grasping tools: Effects of task and apraxia. Neuropsychologia. 47:497–505.

Reynaud E, Lesourd M, Navarro J, Osiurak F. 2016. On the neurocognitive origins of human tool use: A critical review of neuroimaging data. Neurosci Biobehav Rev.

Reynaud E, Navarro J, Lesourd M, Osiurak F. 2019. To Watch is to Work: a Review of NeuroImaging Data on Tool Use Observation Network. Neuropsychol Rev. 29:484–497.

Rossetti Y, Revol P, McIntosh R, Pisella L, Rode G, Danckert J, Tilikete C, Dijkerman HC, Boisson D, Vighetto A, Michel F, Milner AD. 2005. Visually guided reaching: bilateral posterior parietal lesions cause a switch from fast visuomotor to slow cognitive control. Neuropsychologia. 43:162–177.

Salazar-López E, Schwaiger BJ, Hermsdörfer J. 2016. Lesion correlates of impairments in actual tool use following unilateral brain damage. Neuropsychologia. 84:167–180.

Schwartz MF, Kimberg DY, Walker GM, Brecher A, Faseyitan OK, Dell GS, Mirman D, Coslett HB. 2011. Neuroanatomical dissociation for taxonomic and thematic knowledge in the human brain. Proc Natl Acad Sci U S A. 108:8520–8524.

Sirigu A, Cohen L, Duhamel J-R, Pillon B, Dubois B, Agid Y. 1995. A Selective Impairment of Hand Posture for Object Utilization in Apraxia. Cortex. 31:41–55.

Sirigu A, Duhamel J-R, Poncet M. 1991. The role of sensorimotor experience in object recognition. Brain. 114:2555–2573.

Talairach J, Tournoux P. 1988. Co-Planar Stereotaxis Atlas of the Human Brain, Direct.

Tarhan LY, Watson CE, Buxbaum LJ. 2015. Shared and Distinct Neuroanatomic Regions Critical for Tool-related Action Production and Recognition: Evidence from 131 Left-hemisphere Stroke Patients. J Cogn Neurosci. 27:2491–2511.

Thye M, Geller J, Szaflarski JP, Mirman D. 2021. Intracranial EEG evidence of functional specialization for taxonomic and thematic relations. Cortex. 140:40–50.

Tunik E, Frey SH, Grafton ST. 2005. Virtual lesions of the anterior intraparietal area disrupt goal-dependent on-line adjustments of grasp. Nat Neurosci. 8:505–511.

Ungerleider LG, Mishkin L. 1982. Two cortical visual systems. In: Ingle DJ,, Goodale MA,, Mansfield RJW, editors. Analysis of visual behavior. Cambridge: MIT Press. p. 549–586.

Van Essen DC. 2005. A Population-Average, Landmark- and Surface-based (PALS) atlas of human cerebral cortex. Neuroimage. 28:635–662.

Vingerhoets G, Clauwaert A. 2015. Functional connectivity associated with hand shape generation: Imitating novel hand postures and pantomiming tool grips challenge different nodes of a shared neural network. Hum Brain Mapp. 36:3426–3440.

Whitfield-Gabrieli S, Nieto-Castanon A. 2012. Conn : A Functional Connectivity Toolbox for Correlated and Anticorrelated Brain Networks. Brain Connect. 2:125–141.

Wurm MF, Caramazza A, Lingnau A. 2017. Action Categories in Lateral Occipitotemporal Cortex Are Organized Along Sociality and Transitivity. J Neurosci. 37:562–575.

Yee E, Drucker DM, Thompson-Schill SL. 2010. fMRI-adaptation evidence of overlapping neural representations for objects related in function or manipulation. Neuroimage. 50:753–763.